Journal of Molecular Structure 1200 (2020) 127084

Contents lists available at ScienceDirect

Journal of Molecular Structure

journal homepage: http://www.elsevier.com/locate/molstruc

Synthesis, crystal structures and biological evaluation of new pyridazine derivatives

Bholey Singh [a], Rohit Bhatia [c], Balaram Pani [a], Deepak Gupta [a, b, *]

[a] Department of Chemistry, Bhaskaracharya College of Applied Sciences (University of Delhi), Sector-2, Dwarka, New Delhi, 110075, India
[b] Present Address: Institut de La Matie're Condense et des Nanosciences (IMCN), Universite' Catholique de Louvain (UCL), Place Louis Pasteur 1, 1348, Louvain-la-Neuve, Belgium
[c] Rudraksh Proudhyogiki Sangathan, Delhi, India

ARTICLE INFO

Article history:
Received 13 May 2019
Received in revised form
12 September 2019
Accepted 15 September 2019
Available online 18 September 2019

Keywords:
Anti-biotic
Crystal
Diels-alder
Pyridazine
Tetrazine

ABSTRACT

A series of functionalized pyridazine derivatives (**1**–**10**) *4-phenyl-3,6-di(pyridine-4-yl)pyridazine* (***1***), *3-(3,6-di(pyridin-4-yl)pyridazin-4-yl)aniline* (***2***), *4-(pyridin-3-yl)-3,6-di(pyridin-4-yl)pyridazine* (***3***), *3,6-di(pyridin-4-yl)-4-(thiophen-2-yl)pyridazine* (***4***), *6-methyl-1,4-di(pyridin-4-yl)-5H-pyrrolo[3,4-d]pyridazine-5,7(6H)-dione* (***5***), *4-phenyl-3,6-di(pyridine-3-yl)pyridazine* (***6***), *3-(3,6-di(pyridin-4-yl)pyridazin-3-yl)aniline* (***7***), *3,4,6-tri(pyridin-3-yl)pyridazine* (***8***), *3,6-di(pyridin-3-yl)-4-(thiophen-2-yl)pyridazine* (***9***), *6-methyl-1,4-di(pyridin-3-yl)-5H-pyrrolo[3,4-d]pyridazine-5,7(6H)-dione* (***10***) were synthesized by one-step methodologies which also include *Inverse Electron Demand Diels-Alder* reaction. The compounds were isolated in high yields without any tedious purification procedures and characterized by NMR, Mass spectrometry, Elemental Analysis and X-ray diffraction techniques. The crystal structures of five compounds were studied. The pyridazines were subjected to anti-microbial evaluations where few of the compounds showed moderate to high activity against most of the bacteria and fungi presented in this study.

1. Introduction

Nitrogeneous heterocyclic compounds such as tetrazines are known as efficient photo– and redox– active compounds, which have found applications in variety of areas such as dyes, bio-activity, non-linear optics and light emission [1–3]. Considered as highly electron-poor aromatic system, tetrazine-based compounds are also being developed for electron-storage and photo-oxidation [4,5]. Aiming for significant utilization of tetrazines in material science and intrigued by such properties, polytetrazines and tetrazine-containing polymers and covalent organic frameworks are also coming-up with promising applications [6–8]. Moreover, tetrazine moiety has also been elegantly deployed as a part of ligand system in coordination chemistry in the form of supramolecular coordination complexes and metal-organic framework [9,10]. In these systems, the tetrazine unit acts as a functional building block and play diverse roles such as site for multiple-electron uptake and appending various functional units (application oriented functionalization). Tetrazine platform have also been employed as synthetic intermediates as well as starting material in several natural product synthesis *via* tetrazine to pyridazine conversion [11]. Pyridazines belong to the family of diazine compounds containing two sp^2-hybridized adjacent nitrogen atoms. The pyridazine derivatives have been widely studied as biologically-active compounds particularly for their antimicrobial activities [12–15]. Functionalized pyridazines unit containing compounds have been identified as highly electron deficient compounds which prompted their utilization as electrochromic materials and in metal-organic frameworks [16,17]. In order to improve the existing properties and to generate new functions of nitrogen-based materials, modification of the tetrazine unit to functionalized pyridazines is extremely useful.

In the last few decades, a number of synthetic strategies such as Cu-catalyzed azide-alkyne based “click reaction” and Diels-Alder reactions have been developed as versatile tools for the conjugation of molecules *via* carbon-carbon bond formation. Among these, iEDDA (inverse Electron Demand Diels–Alder) reaction has been

* Corresponding author. Department of Chemistry Institution, Bhaskaracharya College of Applied Sciences (University of Delhi), Sector-2, Dwarka, New Delhi, 110075, India.
E-mail addresses: deepakg2003@gmail.com, deepak.gupta@uclouvain.be (D. Gupta).

https://doi.org/10.1016/j.molstruc.2019.127084
0022-2860/

introduced and gained importance as potential click reaction scheme involving a 1,2,4,5−tetrazine and olefins [18]. It has emerged as a metal-free route for bio-orthogonal substrate labelling which offers fast reactivity (even at RT), clean products and compatibility [19−21]. Very recently, this reaction platform has been applied to append pyridazines on DNA [22]. Herein, we report on a series of functionalized pyridazines derived from the reaction of tetrazine compounds with various functional units *via* the single step iEDDA approach. All the pyridazines have been thoroughly characterized and studied for their anti-biotic properties such as anti-bacterial and anti-fungal.

2. Results and discussion

The *inverse-electron demand Diels-Alder* (iEDDA) reaction has been widely employed to append organic unit/s on a variety of tetrazines by converting the tetrazine into a substituted pyridazine. The reaction requires normal reflux conditions to react a tetrazine moiety with the organic unit to be appended without using any external reagent. The water-based work-up of these reactions provide clean products in high yields. Owing to the fast reaction kinetics, this reaction has been widely utilized to append biological as well as luminescent molecules on tetrazine moiety containing building blocks [23]. Therefore, as compared to the Copper-based "click reactions", the implementation of iEDDA reaction of tetrazines is one of the excellent methodologies to achieve pyridazine-based compounds where a number of photo-, redox- and biologically active units can be appended on the pyridazine ring in one step.

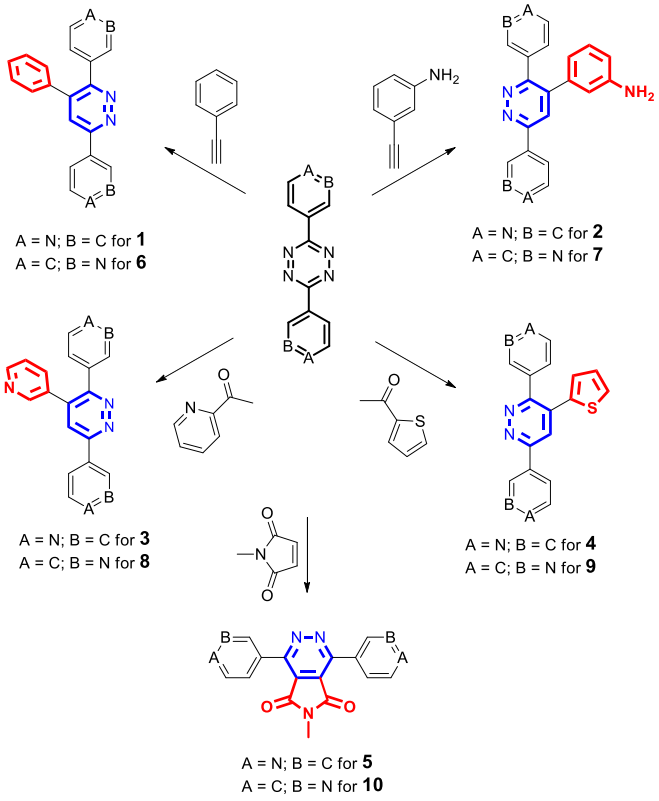

Scheme 1. One-step synthesis of pyridyl-functionalized pyridazines **1**−**10**.

2.1. Synthesis of functionalized pyridazines

The pyridazine derivatives **1**, **2**, **5**, **6**, **7** and **10** were synthesized by single step procedure using the *iEDDA* reaction between tetrazine ring of the di-3,6-(4-pyridyl)-1,2,4,5-tetrazine/di-3,6-(3-pyridyl)-1,2,4,5-tetrazine precursor with acetylene-based dienophiles (phenylacetylene for **1** and **6**; 3-aminophenylacetylene for **2** and **7**) and *N*-methylmaleimide for **5** and **10** in DMF followed by extraction in DCM resulting in off-white to light yellow colored compounds (Scheme 1). All the compounds were obtained in more than 80% yield. The compounds were found to be soluble in most of the polar organic solvents. The X-ray quality single crystals of the pyridazines were grown by slow evaporation of DCM. The compounds were analyzed with the help ^{1}H NMR, ^{13}C NMR, 2D-COSY, Mass spectrometry, single crystal X-ray diffraction and elemental analysis.

The pyridyl functionalized pyridazines **3**, **4**, **8** and **9** were obtained by a slightly different procedure where 2-acetylpyridine for **3** and **8**, 2-acetylthiophene for **4** and **9** were reacted with dipyridyltetrazine precursor in the presence of 2.5% methanolic solution of KOH at RT (Scheme 1). Refluxing these overnight resulted in brown color solutions which on solvent removal produced light yellow to light brown color powder/semi-solid. The products were suspended in water and extracted with DCM. Fine crystals of the products were obtained by slow evaporation of the DCM solution. All the products are soluble in most of the polar organic solvents resulting in clear colorless solutions.

2.2. Characterization

The HRMS data for all the pyridazine compounds (**1**−**10**) was found to be in accordance with the calculated values (*m*/*z* = 311.1282 for **1**; 326.1399 for **2**; 312.1247 for **3**; 317.0848 for **4**; 318.0865 for **5**; 311.1305 for **6**; 326.1405 for **7**; 312.1248 for **8**; 317.0871 for **9**; 318.0995 for **10**) (see SI). The molecular ion peaks were identified and assigned according to the theoretical mass values. The elemental analysis data further justified the high purity of all the compounds. The ^{1}H NMR spectra of the 4-pyridyl-functionalized pyridazines **1**−**5** were recorded in $CDCl_3$. The peak position and integration ratios established the formation of functional group appended pyridazines in pure form with the formation of a single isomer in all the cases (Fig. 1). The four distinct doublets in the aromatic region corresponds to the four pyridyl ring protons which appears in the region (7.3−8.9 ppm) due to asymmetrical structure.

The signal for the only pyridazine ring proton H^{5} can be seen as singlet at different positions between 7.8 and 8.3 ppm for different compounds which justifies the indirect effect of the pendant group on the pyridazine ring whereas the signals for protons of the functional group (phenyl, aniline, thiophenyl and pyridyl) appeared in their usual positions without any major shift in the peak positions in all the compounds. The assignment of the peaks was aided by H−H CoSy data. The correlations were observed for H2−H3 and H2′−H3'. The NH proton in **2** can be seen at 5.25 ppm as broad singlet. The ^{13}C NMR data also supported the products formation.

The ^{1}H NMR spectra of 3-pyridyl functionalized pyridazines **6**−**10** were also recorded in $CDCl_3$ which showed entirely different pattern as compared to NMR spectra of 4-pyridyl functionalized pyridazines (Fig. 2). The peaks were assigned on the basis of CoSy NMR spectra of all the compounds. In the ^{1}H NMR spectra, the signals for the H2 protons of the two pyridyl rings being nearest to the pyridyl nitrogen and the pyridazine unit are most down-fielded and appear at around 9.3 and 8.8 ppm for different compounds. The next appearing peaks could be assigned to the H6 and H6' protons of the two pyridyl rings. The lone pyridazine ring proton (Hα) signal appeared at around similar position (7.9 ppm) in all the NMR spectra. The subsequent peaks in the high field aromatic region

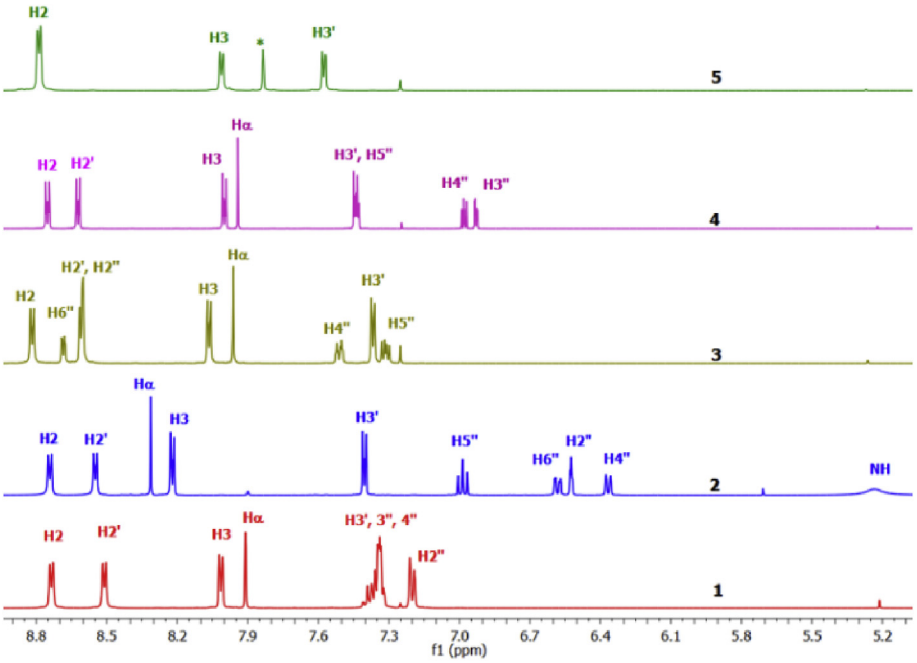

Fig. 1. ^{1}H NMR spectra of functionalized pyridazines **1**–**5** ($CDCl_3$, RT, 400 MHz).

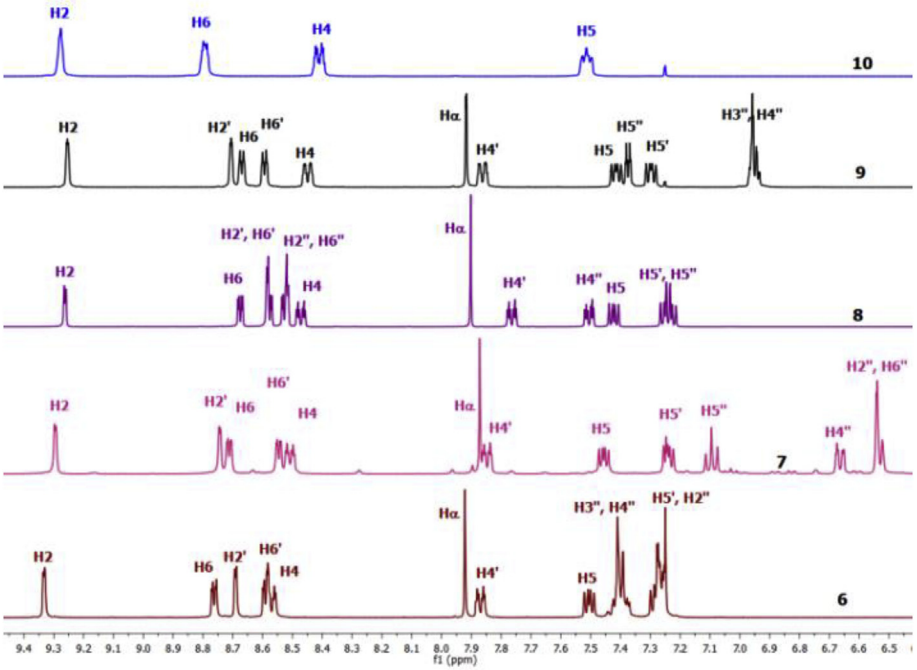

Fig. 2. ^{1}H NMR spectra of functionalized pyridazines **6**–**10** ($CDCl_3$, RT, 400 MHz).

could be easily assigned to the other pendant group on the pyridazine ring. Notably, the signal for the Hα proton in **10** was found absent unlike other pyridazines (**6**–**9**) further establishing the structure of the compound.

2.3. Crystal structure

The X-ray diffraction quality single crystals of five out of the ten functionalized pyridazine compounds **2**, **3**, **6**, **8** and **9** were found to be suitable to X-ray diffraction studies and collected by slow evaporation of a saturated DCM solution at RT (Table 2). Fine quality colorless crystals were decanted and exposed to X-rays on a diffractometer. The crystal structures of the pyridazine compounds resemble; featuring the central pyridazine ring containing the pendant functional group at the fourth position (aniline for **2**, phenyl for **6**, pyridyl for **3** & **8**, thiophenyl **9**) and two 4-pyridyl units (for **2**, **3**) and 3-pyridyl units (for **6**, **8** and **9**) at the third and sixth positions respectively (Fig. 3). The bond length data

Table 1
The dihedral angles between various rings (shown here) and the pyridazine ring in all the crystal structures.

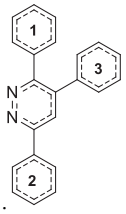

Code	Ring 1	Ring 2	Ring 3
2	49.48	35.78	53.09
3	45.10	21.63	39.36
6	49.67	1.57	53.51
8	54.42	2.40	55.12
9	74.76	14.75	9.17

The values are in degree (°).

showed that the pyridazine rings in all the compounds contain the normal N=N bond (1.31–1.34 Å). Unlike the pyridine substituents, the bond length data of various bonds in the pyridazine ring in all the five crystal structures do not reflect uniformity but lie within the range of the normal pyridazine bond lengths and therefore confirms the electron density delocalization in the ring. The three substituents on the pyridazine ring namely, two pyridyl and the functional group are not co-planar and exist in different orientations (Table 1). One common feature in the crystal structures is the slight tilt of one of the pyridyl rings (ring 1) which is close to the pendant functional group (ring 3) where the angle between the C3 carbon of the pyridyl ring and the nearest pyridazine nitrogen is in the range *ca.* 112°–114° which is less than the normal bond angle found in the parent tetrazine compounds. The crystal structure of **6** is isostructural with the structures presented previously, though the temperature of collections of data sets are different [24,25].

Non-covalent interactions play pivotal role in numerous biological phenomenon where molecules interact in the form of loose aggregates to generate supramolecules. These weaker supramolecular interactions form the core of crystal engineering and are therefore essential [26]. Interestingly, all the crystal structures shown in the present study display a variety of non-covalent interactions such as H-bonding and $\pi-\pi$ stacking in the crystal structures (Figs. 4 and 5). To mention a few, compound **2** shows a rather strong network of inter-molecular H-bonding interactions which extend along the *b*-axis where one of the $-NH_2$ hydrogens of pendant aniline ring is interacting with the pyridazine nitrogen (~2.3 Å) of the adjacent molecule in the same direction while the other one is involved with pyridyl nitrogen (~2.4 Å) of different molecule in the other direction. The molecules of compound **3**

Table 2
Crystallographic data for compounds **2**, **3**, **6**, **8** and **9**.

Sample Code	2	3	6	8	9
Chemical Formula	C20H15N5	C19H13N5	C20H14N4	C19H13N5	C18H12N4S
Formula Mass	325.37	311.34	310.35	311.34	316.38
Crystal System	Monoclinic	Orthorhombic	Monoclinic	Monoclinic	Orthorhombic
a/Å	19.2721(16)	7.3813(3)	14.3445(10)	14.3445(6)	5.3569(3)
b/Å	8.1066(7)	10.6853(4)	7.1214(4)	7.0963(3)	16.5036(8)
c/Å	10.3200(7)	38.6185(16)	15.8417(10)	15.4880(7)	16.8191(8)
α/°	90.0000	90.0000	90.0000	90.0000	90.0000
β/°	99.887(7)	90.0000	105.483(7)	104.798(5)	90.0000
γ/°	90.0000	90.0000	90.0000	90.0000	90.0000
Unit Cell Volume/Å	1588.4(2)	3045.9(2)	1559.55(18)	1524.28(12)	1486.95(13)
Temperature/K	293	293	293	293	293
Space Group	P 21/c	*P*bca	P 21/n	P 21/n	P 21 21 21
No. of formula unit per unit cell, Z	4	8	4	4	4
Density (g cm^{-3})	1.361	1.358	1.322	1.357	1.413
F(000)	680	1296.0	648.0	648.0	656.0
No. of reflections measured	22050	24386	22268	22304	21688
No. of independent reflections	3968	3938	3957	3910	3766
Observed [$I > 2\sigma(I)$] reflections	4279	23257	23257	5679	4911
R [$F^2 > 2\sigma(F^2)$], w*R*(all data)	0.0646, 0.1738	0.0612, 0.1684	0.0555, 0.0917	0.0489, 0.1340	0.0467, 0.1175
S	1.041	1.066	1.030	1.015	1.056

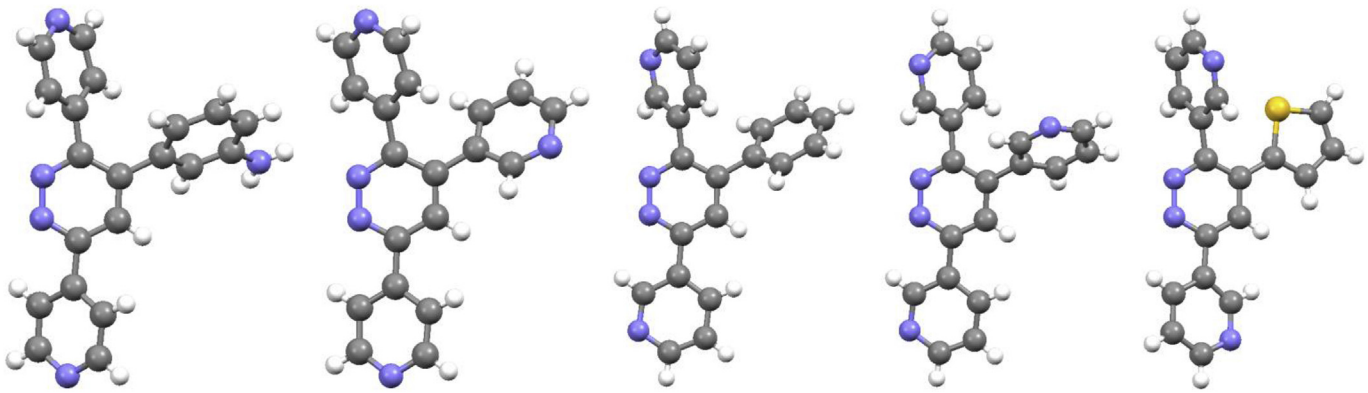

Fig. 3. Crystal structures of functionalized pyridazines **2**, **3**, **6**, **8** & **9**. Grey: C, Blue: N, White: H, Yellow: S.

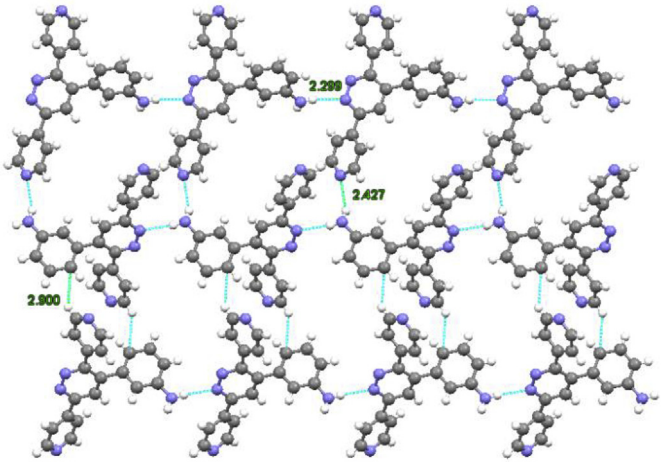

Fig. 4. Network of hydrogen-bonding and CH−π interaction formed molecules of **2**.

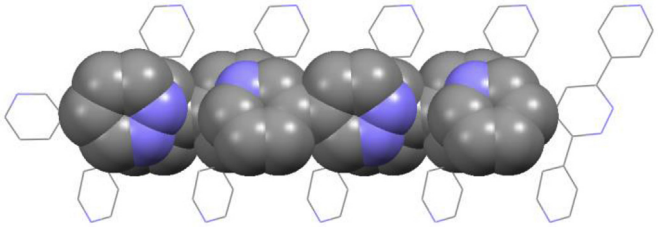

Fig. 5. Inter-molecular π−π stacked arrangement of pyridyl rings in crystal structure of **3**.

undergo intermolecular π-π stacking interactions.

In the crystal structure of **3**, the 3-pyridyl ring is stacked over the electron deficient pyridazine ring of the adjacent molecule leading to an offset packing forming a linear chain in a *hand-shake* manner along the *a*-axis. These linear chains are inter-connected through H-bonds and thus stabilize the crystal packing structure. Thus the ability to make intermolecular networks and linear chains induces an additional feature to these compounds to become suitable for making supramolecular coordination structures when bonded with metal-ions.

The absorption properties of all the pyridazines (**1**–**10**) were studied by using UV–Vis absorption spectroscopy in dichloromethane solution at room temperature. All the compounds show intense bands in UV region which can be assigned to the aromatic ring based transitions. The molar extinction coefficients were in the range of 15000–90000 $M^{-1}cm^{-1}$ in UV region (see supporting information). No significant absorption was found in the visible region (see Fig. 6).

2.4. Antimicrobial activity

The in-vitro antimicrobial activity for the synthesized compounds was determined against various bacteria e.g. *E. coli*, *S. aureus, P. aeruginosa, K. pneumonia and B. subtilis* as average diameter of the inhibition zone in mm whereas the antifungal activity was estimated against *R. solani*, *S. rolfsii*, *F. oxysporum* and *A. niger*. These data are shown in Tables 3 and 4. All the compounds showed dose response behavior and possessed moderate to good activity against both gram negative and gram positive bacteria in comparison to the standard against tested bacteria. In case of *E. coli* and *P. aeruginosa*, **4** was found to be least active whereas **2**, **3**, **7** and

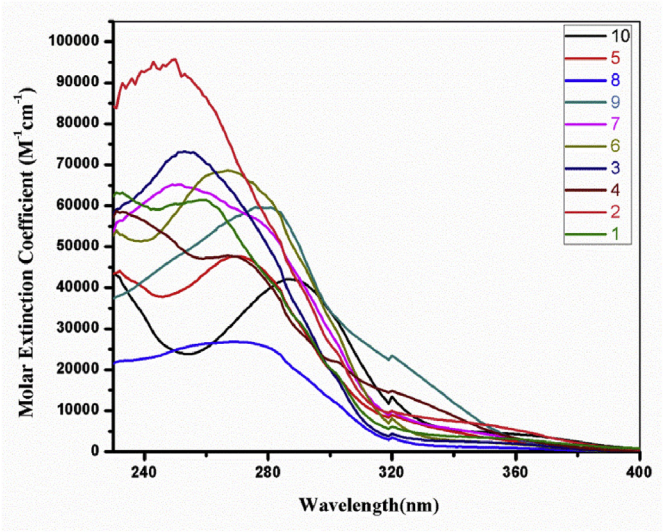

Fig. 6. Absorption spectra of functionalized pyridazine compounds (**1**–**10**).

9 were most active in comparison to the standard respectively. For *S. aureus*, functionalized-pyridazine **7** was most active whereas **1** and **4** were least active. Similar trend was observed in case of *K. pneumonia* where again **4** displayed least activity and **9** was most active. In case of *B. subtilis*, **1** was seen to be least active while **7** showed highest active in comparison to standard among all. Similar to the anti-bacterial studies, all pyridazines showed dose response behavior and possess moderate activity in comparison to the standard against tested Fungi. Compound **3** and **8** were found to be most active against in case of *R. solani* whereas the rest of compounds showed average to moderate activity. In case of *S. rolfsii*, **2** were least active and **7** was most active whereas **8** displayed highest activity against *F. oxysporum*, In case of *A. niger*, most of the pyridazines showed poor activity but **3** showed moderate activity (see Table 4).

2.4.1. Materials and methods

All the starting materials and solvents were purchased from local vendors and utilized without any purification. All the solvents were dried and distilled using general procedures prior to reactions. The reactions were carried out in air-atmosphere. The NMR spectra were collected on Bruker Avance-400 spectrometer using TMS as internal standard. The absorption spectra were recorded on an Analytikjena Spectrophotometer (specord 250). The crystals were mounted on Oxford Xcalibur Nova X-ray diffractometer with a four circle κ Goniometer employing a graphite monochromatized MoKα. Single crystal X-ray data was recorded on Oxford callibur Sapphire3 diffractometer employing a graphite monochromatized MoKα at room temperature. The data of all the crystals was reduced using CrysAlis pro software available with the diffractometer and thereby reduced the Rint. Further least square refinement after introduction of anisotropic displacement parameters yielded the R values mentioned in Table 2. Elemental Analysis were carried out on Flash EA series 1112 CHNS analyser. The ESI MS data was collected from a Agilent Technologies 6530 Accurate-Mass Q-TOF LC/MS. Fungal culture of *R. solani* (ITCC 4502), *S. rolfsii* (ITCC 6263) F. oxysporum (ITCC 4884) and *A. niger* (ITCC 1624) were obtained from the Indian type culture collection, Division of Mycology and Plant Pathology, Indian Agricultural Research Institute (IARI), New Delhi. Bacterial culture *E. coli* (MTCC 443), *Staphylococcus aureus* (MTCC 3160), *Pseudomonas aeruginosa* (MTCC 2581), B. subtilis (MTCC 441) and *Klebsiella pneumoniae* (MTCC 7028) were procured

Table 3
Antimicrobial screening results of few of the synthesized compounds (**1**–**9**).

Code	*E. coli* Zone of inhibition (mm)					*S. aureus* Zone of inhibition (mm)					*P. aeruginosa* Zone of inhibition (mm)					*K. pneumonia* Zone of inhibition (mm)					*B. subtilis* Zone of inhibition (mm)				
	200	100	50	25	12.5	200	100	50	25	12.5	200	100	50	25	12.5	200	100	50	25	12.5	200	100	50	25	12.5
1	20	19	16	13	–	23	18	15	09	–	29	24	19	16	11	21	15	12	06	–	18	16	13	10	05
2	27	24	19	15	08	30	27	21	19	14	31	26	19	14	09	25	21	16	13	08	22	18	14	07	–
3	33	29	24	19	11	31	26	21	16	09	29	24	17	11	07	17	11	08	–	–	24	16	12	06	–
4	21	17	13	–	–	23	19	14	07	–	19	15	07	–	–	14	09	–	–	–	20	16	12	08	–
6	31	29	23	19	15	32	28	22	14	08	27	24	16	09	–	23	16	11	09	05	19	15	11	09	06
7	34	28	21	17	14	35	30	24	21	19	30	26	23	19	15	28	23	19	14	08	26	21	16	11	08
8	30	25	19	16	12	28	20	14	08	–	28	23	17	13	09	21	19	16	14	09	23	18	15	12	08
9	29	23	17	14	10	29	26	21	18	12	32	28	21	18	14	27	23	18	15	11	24	19	16	07	–
Control	37	35	32	30	26	38	33	30	28	26	39	34	32	30	28	32	30	29	27	25	28	26	25	23	19

Table 4
Anti-fungal screening results of few of the synthesized compounds (**1**–**9**).

Code	Fungal inhibition (%)															
	R. solani				*S. rolfsii*				*F. oxysporum*				*A. niger*			
	100	50	25	12.5	100	50	25	12.5	100	50	25	12.5	100	50	25	12.5
1	51	48	41	22	53	42	21	14	42	39	30	25	51	41	31	29
2	38	29	14	5	33	30	28	15	40	36	25	19	43	36	26	15
3	83	79	73	61	71	69	62	57	87	78	69	57	84	71	69	49
4	77	68	52	41	65	55	51	47	82	74	69	59	79	66	57	44
6	81	74	67	56	76	66	47	31	83	77	68	42	68	44	36	19
7	67	59	47	36	79	64	56	42	55	47	41	39	77	63	54	43
8	84	71	62	53	77	71	63	51	88	78	67	52	80	76	64	48
9	45	39	33	25	52	43	36	27	61	53	45	34	58	45	39	21
Standard	92	84	77	73	85	83	75	72	93	86	79	71	94	85	76	69

from the microbial type culture collection and gene bank, Institute of Microbial Technology, Chandigarh.

2.4.2. Poison food assay

Antifungal assay was carried out by a poisoned food technique using potato-dextrose-agar (4% PDA) medium against four phyto-pathogenic fungi *Rhizoctonia solani*, *Sclerotium rolfsii, Fusarium oxysporum* and *A. niger* at different concentrations (200–12.5 ppm) [27]. 1 mL of stock solution was added to 50 mL of PDA medium in to obtain desired concentrations. The medium was then poured into two Petri plates under aseptic conditions in a laminar flow chamber. Similarly other concentrations were prepared by serial dilution process. 1 mL of methanol was used as a control. A 5 mm thick disc of fungus was put at the center of the medium in the test petri plate and the plates were kept in BOD incubator at 28 ± 1 °C till the fungal growth in the control dishes was completed (6–10 days). The mycelial growth (cm) in both treated (T) and control (C) petri-plates use measured diametrically in three different directions. From the mean growth of above readings, percentage inhibition of growth (I) was calculated by using the following equation:

$$\text{Percent growth } \textit{inhibition } I(\%) = [(T - C)/C] \times 100$$

EC_{50} (effective concentration for 50% inhibition of mycelial growth) was calculated from the percent inhibition (IC) as per the following equations:

$$IC = [(\% I - C \cdot F.) / (100 - C \cdot F.)] \times 100$$

$$C.F.\ (\text{Correction Factor}) = [(90 - C)/C] \times 100$$

where 90 is the diameter of the petri dishes (mm) and C is the growth of the fungus (mm) in control. EC_{50} (mgL^{-1}) was calculated from the concentration (mgL^{-1}) and corresponding IC data of each compound with the help of statistical package (GW BASIC) [24].

2.4.3. Disk diffusion assay

The antimicrobial potential of synthesized metal complexes was tested using a disk diffusion assay. Briefly the nutrient agar medium (25 mL) was poured into petri dishes (90 mm in diameter) under aseptic conditions in a laminar flow hood. The plates were kept in the laminar flow chamber for solidification of the media. After solidification 100 μL of fresh culture (log phase) was spread on the surface of the solidified medium with the help of a spreader. The plates were then kept in laminar flow for drying. Once dried, five plain sterile disks were placed in the plate and 5 μL of test solution of different concentration (200–12.5 ppm) was loaded on each disk. In control plate, commercially procured ampicillin (10 μg/disk) was used. Plates were then kept at 37 °C for 24 h in the incubator and zone of inhibition (in mm) was recorded for all the compounds tested and commercial antibiotic. All experiments were performed in triplicate for each treatment against each bacteria.

2.4.4. Experimental section

*2.4.4.1. General procedure for the preparation of functionalized pyridazines (**1**, **2**, **5**, **6**, **7**, **10**).* In a round bottom flask, di-3,6-(4-pyridyl)-1,2,4,5–tetrazine (1 mmol) for **1**, **2** & **5** or di-3,6-(3-pyridyl)-1,2,4,5–tetrazine (1 mmol) for **6**, **7** & **10** was suspended in DMF at 100 °C with stirring. After half an hour, phenylacetylene for **1**, **6**; 3-ethynylaniline for **2**, **7**; *N*-methylmaleimide for **5**, **10** (1 mmol) was added to the reaction mixture. This was left for stirring. The formation of product was monitored by TLC. The light brown color reaction mixture was poured into ice-cold water which was washed with 40 × 3 mL DCM. Solvent layer was evaporated on a rotary evaporator to obtain the desired product as light yellow solids.

*2.4.4.2. Synthesis of 4-phenyl-3,6-di(pyridine-4-yl)pyridazine (**1**).* Prepared from phenylacetylene, light yellow crystal, yield = 88.6%, mp = 190.8 °C; MS: (*m*/*z*) 311.1282 (MH^+); ^1H NMR ($CDCl_3$, 400 MHz, δ): 8.74 (dd, 2H, *J* = 4Hz, H2), 8.51 (dd, 2H, *J* = 4Hz, H2'), 8.014 (dd, 2H, *J* = 4 Hz, H3), 7.91 (s, 1H, Hα), 7.39–7.32 (m, 5H, H3′,3″,4″), 7.21–7.19 (m, 2H, H2″). Anal. Calcd. for $C_{20}H_{14}N_4$: C, 77.40; H, 4.55; N, 18.05. Found: C, 77.52; H, 4.34; N, 18.14.

*2.4.4.3. Synthesis of 3-(3,6-di(pyridin-4-yl)pyridazin-4-yl)aniline (**2**).* Prepared from 3-ethynylaniline, light yellow crystal, yield = 92.3%, mp = 212 °C; MS: (*m*/*z*) 326.1399 (MH^+); ^1H NMR ($CDCl_3$, 400 MHz, δ): 8.74 (d, 2H, *J* = 4 Hz, H2), 8.55 (d, 2H, *J* = 4 Hz, H2'), 8.31 (s, 1H, Hα), 8.22 (d, 2H, *J* = 4 Hz, H3), 7.40 (d, 2H, *J* = 4 Hz, H3'), 6.99 (t, 1H, H5″), 6.58 (d, 1H, *J* = 4 Hz, H6″), 6.52 (m, 1H, H2″), 6.37 (d, 1H, *J* = 4 Hz, H4″), 5.23 (broad singlet, 2H, NH). Anal. Calcd. for $C_{20}H_{15}N_5$: C, 73.83; H, 4.65; N, 21.52. Found: C, 73.98; H, 4.48; N, 21.54.

*2.4.4.4. Synthesis of 6-methyl-1,4-di(pyridin-4-yl)-5H-pyrrolo[3,4-d] pyridazine-5,7(6H)-dione (**5**).* Prepared from *N*-methylmaleimide, off-white crystal, yield = 78.5%, mp = 205.6 °C; MS: (*m*/*z*) 318.0995 (MH^+). ^1H NMR ($CDCl_3$, 400 MHz, δ): 8.78 (d, 4H, *J* = 4 Hz, H2), 8.01 (d, 2H, *J* = 4 Hz, H3), 7.57 (d, 2H, H5), 8.22 (d, 2H, *J* = 4 Hz, H3'), 2.50 (s, 3H, *N*-methyl). Anal. Calcd. for $C_{17}H_{11}N_5O_2$: C, 64.35; H, 3.49; N, 22.07. Found: C, 64.42; H, 3.42; N, 21.94.

*2.4.4.5. Synthesis of 4-phenyl-3,6-di(pyridine-3-yl)pyridazine (**6**).* Prepared from phenylacetylene, off-white crystal, yield = 84.4%, mp = 183.8 °C; MS: (*m*/*z*) 311.1305 (MH^+); ^1H NMR ($CDCl_3$, 400 MHz, δ): 9.33 (s, 1H, H2), 8.76 (d, 1H, H6), 8.69 (s, 1H, H2'), 8.60–8.56 (m, 2H, H6', H4), 7.92 (s, 1H, Hα), 7.87 (dd, 1H, H4'), 7.52–7.49 (dd, 1H, H5), 7.42–7.37 (m, 3H, H3″, H4″), 7.30–7.25 (m, 3H, H5', H2″). Anal. Calcd. for $C_{20}H_{14}N_4$: C, 77.40; H, 4.55; N, 18.05. Found: C, 77.49; H, 4.53; N, 17.98.

*2.4.4.6. Synthesis of 3-(3,6-di(pyridin-4-yl)pyridazin-3-yl)aniline (**7**).* Prepared from 3-ethynylaniline, off-white crystal, yield = 91.2%, mp = 204.4 °C; MS: (*m*/*z*) 326.1405 (MH^+); ^1H NMR ($CDCl_3$, 400 MHz, δ): 9.29 (s, 2H, *J* = 4 Hz, H2), 8.74 (2, 2H, *J* = 4 Hz, H2'), 8.71 (d, 1H, H6), 8.54 (d, 1H, H6'), 8.50 (d, *J* = 4 Hz, 1H, H4), 7.87 (s, 1H, Hα), 7.85 (d, *J* = 4 Hz, 1H, H4'), 7.47–7.44 (dd, *J* = 4 Hz, 1H, H5), 7.25–7.22 (m, 1H, H5'), 7.10 (t, 1H, H5″), 6.66 (d, 1H, H4″), 6.54 (s, 1H, H2″), 6.52 (d, 1H, H6″). Anal. Calcd. for $C_{20}H_{15}N_5$: C, 73.83; H, 4.65; N, 21.52. Found: C, 73.94; H, 4.55; N, 21.51.

*2.4.4.7. Synthesis of 6-methyl-1,4-di(pyridin-3-yl)-5H-pyrrolo[3,4-d] pyridazine-5,7(6H)-dione (**10**).* Prepared from *N*-methylmaleimide, off-white crystal, yield = 80.4%, mp = 183.2 °C; MS: (*m*/*z*) 318.0995 (MH^+). ^1H NMR ($CDCl_3$, 400 MHz, δ): 9.28 (s, 2H, H2), 8.79 (m, 2H, H6), 8.43–8.39 (m, 2H, H4), 7.52 (t, 2H, H5). Anal. Calcd. for $C_{17}H_{11}N_5O_2$: C, 64.35; H, 3.49; N, 22.07. Found: C, 64.46; H, 3.41; N, 21.98.

*2.4.4.8. General procedure for the preparation of functionalized pyridazines (**3**, **4**, **8**, **9**).* In a round bottom flask, di-3,6-(4-pyridyl)-1,2,4,5−tetrazine (for **3** & **4**)/di-3,6-(3-pyridyl)-1,2,4,5−tetrazine (for **8** & **9**) (1 mmol) and 2-acetylpyridine (for **3** & **8**)/2-acetylthiophene (for **4** & **9**) (1 mmol) were suspended in methanol at 65 °C with stirring. To this, 1 mL of 2.5% methanolic solution of KOH was added to the reaction mixture. This was left for stirring. The formation of product was monitored by TLC. The solvent was reduced under vacuum. The brown color reaction mixture was poured into ice-cold water which was washed with 40 × 3 mL DCM. Solvent layer was evaporated on a rotary evaporator to obtain the desired product as light yellow/off-white solids.

*2.4.4.9. Synthesis of 4-(pyridin-3-yl)-3,6-di(pyridin-4-yl)pyridazine (**3**).* Prepared from 3-acetylpyridine, light yellow product, yield = 89.6%, mp = 218.3 °C. MS: (*m*/*z*) 312.1247 (MH^+); ^1H NMR ($CDCl_3$, 400 MHz, δ): 8.81 (d, 2H, H2), 8.68 (d, 1H, H6″), 8.60 (d, 3H, H2', H2″), 8.06 (d, 2H, H3), 7.96 (s, 1H, Hα), 7.51 (d, 1H, H4″), 7.36 (d, 2H, H3'), 7.33–7.30 (dd, *J* = 4Hz, 1H, H5″). Anal. Calcd. for $C_{19}H_{13}N_5$: C, 73.30; H, 4.21; N, 22.49. Found: C, 73.46; H, 4.16; N, 22.38.

*2.4.4.10. Synthesis of 3,6-di(pyridin-4-yl)-4-(thiophen-2-yl)pyridazine (**4**).* Prepared from 2-acetylthiophene, off-white product, yield = 85.8%, mp = 225 °C. MS: (*m*/*z*) 317.0848 (MH^+); ^1H NMR ($CDCl_3$, 400 MHz, δ): 8.76–8.74 (dd, *J* = 4Hz, 2H, H2), 8.63–8.61 (dd, *J* = 4Hz, 2H, H2'), 8.00 (dd, *J* = 4Hz, 2H, H3), 7.94 (s, 1H, Hα), 7.44 (dd, *J* = 4Hz, 2H, H3'), 7.43 (d, 1H, H5″), 6.98 (dd, *J* = 4Hz, 2H, H4″), 6.93 (dd, 1H, *J* = 4Hz, 2H, H3″). Anal. Calcd. for $C_{18}H_{12}N_4S$: C, 68.33; H, 3.82; N, 17.71; S, 10.13. Found: C, 68.20; H, 4.06; N, 17.60; S, 10.14.

*2.4.4.11. Synthesis of 3,4,6-tri(pyridin-3-yl)pyridazine (**8**).* Prepared from 3-acetylpyridine, light yellow product, yield = 85.8%, mp = 248.2 °C. MS: (*m*/*z*) 312.1248 (MH^+); ^1H NMR ($CDCl_3$, 400 MHz, δ): 9.26 (d, 1H, H2), 8.67 (dd, *J* = 4Hz, 1H, H6), 8.57 (m, 2H, H2', H6'), 8.53–8.51 (m, 2H, H2″, H6″), 8.49–8.46 (ddd, 1H, H4), 7.9 (s, 1H, Hα), 7.78–7.75 (ddd, 1H, H4'), 7.52–7.49 (ddd, 1H, H4″), 744–7.41 (dd, *J* = 4Hz, 1H, H5), 7.27–7.21 (ddd, 2H, H5', H5″). Anal. Calcd. for $C_{19}H_{13}N_5$: C, 73.30; H, 4.21; N, 22.49. Found: C, 73.42; H, 4.14; N, 22.44.

*2.4.4.12. Synthesis of 3,6-di(pyridin-3-yl)-4-(thiophen-2-yl)pyridazine (**9**).* Prepared from 2-acetylthiophene, off-white product, yield = 87.6%, mp = 251.6 °C. MS: (*m*/*z*) 317.0871 (MH^+); ^1H NMR ($CDCl_3$, 400 MHz, δ): 9.25 (s, 1H, H2), 8.71 (s, 1H, H2'), 8.67 (d, 1H, H2'), 8.59 (d, *J* = 4Hz, 1H, H6), 8.45 (d, 1H, H6'), 7.92 (s, 1H, Hα), 7.86 (d, 1H, H4'), 7.43–7.40 (dd, *J* = 4Hz, 1H, H5), 7.37 (d, 1H, H5″), 7.31–7.28 (dd, *J* = 4Hz, 1H, H5'), 6.97–6.93 (m, 2H, H3″, H4″). Anal. Calcd. for $C_{18}H_{12}N_4S$: C, 68.33; H, 3.82; N, 17.71; S, 10.13. Found: C, 68.26; H, 3.98; N, 17.58; S, 10.18.

Acknowledgement

DG is indebted to Science and Engineering Research Board (India) for a generous funding (YSS/2015/001820) and Bhaskaracharya College of Applied Sciences (University of Delhi) for research facilities. BS thanks UGC for Junior Research Fellowship (162000320). Authors acknowledge scientific support from University Science Instrumentation Center and Department of Chemistry (University of Delhi). Authors thank Dr. Koen Robeyns (Institut de la Matie're Condense et des Nanosciences (IMCN), Universite' Catholique de Louvain, Belgium) for frutiful discussions on improving the crystallography studies.

1878879 (for **2**), 1878881 (for **3**), 1878877 (for **6**), 1881615 (for **8**) and 1882828 (for **9**) contains the supplementary crystallographic data for the respective compounds. These data can be obtained free of charge from the Cambridge Crystallographic Data Centre *via* www.ccdc.cam.ac.uk/data_request/cif.

Appendix A. Supplementary data

Supplementary data to this article can be found online at https://doi.org/10.1016/j.molstruc.2019.127084.

References

[1] A.M. Prokhorov, D.N. Kozhevnikov, Prog. Heterocycl. Chem. 23 (2011)

403–425.
[2] G. Clavier, P. Audebert, Chem. Rev. 110 (2010) 3299–3314.
[3] T. Sasaki, K. Kanematsu, T. Hiramatsu, J. Chem. Soc. Perkin Trans. 1 (1974) 1213–1215.
[4] C.R. Benson, A.K. Hui, K. Parimal, B.J. Cook, C.-H. Chen, R.L. Lord, A.H. Flood, K.G. Caulton, Dalton Trans. 43 (2014) 6513–6524.
[5] E.-J. Macchi, C. Allain, V. Alain-Rizzo, C. Dumas-Verdes, L. Galmiche, J.-F. Audibert, M.B. Desta, R.B. Pansu, P. Audebert, New J. Chem. 38 (2014) 3401–3407.
[6] D.-S. Zhang, Z. Chang, Y.-B. Lv, T.-L. Hu, X.-H. Bu, RSC Adv. 2 (2012) 408–410.
[7] E. Sagot, A.L. Roux, C. Soulivet, E. Pasquinet, D. Poullain, E. Girard, P. Palmas, Tetrahedron 63 (2007) 11189–11194.
[8] Z. Li, J. Ding, Macromol. Chem. Phys. 212 (2011) 2260–2267.
[9] W. Kaim, Coord. Chem. Rev. 230 (2002) 127–139.
[10] G. Nickerl, I. Senkovska, S. Kaskel, Chem. Commun. 51 (2015) 2280–2282.
[11] N. Saracoglu, Tetrahedron 63 (2007) 4199–4236.
[12] K. Neumann, A. Gambardella, A. Lilienkampf, M. Bradley, Chem. Sci. 9 (2018) 7198–7203.
[13] N.G. Kandle, M.I. Mohamed, H. Zaky, H.M. Mohamed, Eur. J. Med. Chem. 44 (2009) 1989–1996.
[14] R.M. Butnariu, I.I. Mangalagiu, Bioorg. Med. Chem. 17 (2009), 2923-2829.
[15] A. Feraldi-Xypolia, D.G. Pardo, J. Cossy, Eur. J. Org. Chem. (2018) 3541–3553.
[16] Q. Ye, W.T. Neo, C.M. Cho, S.W. Yang, T. Lin, H. Zhou, H. Yan, X. Lu, C. Chi, J. Xu, Org. Lett. 16 (2014) 6386–6389.
[17] B. Li, H.-M. Wen, H. Wang, H. Wu, T. Yildirim, W. Zhou, B. Chen, Energy Environ. Sci. 8 (2015) 2504–2511.
[18] R.A. Carboni, R.V. Lindsey Jr., J. Am. Chem. Soc. 81 (1959) 4342–4346.
[19] B.L. Oliveira, Z. Guo, G.J.L. Bernardes, Chem. Soc. Rev. 46 (2017) 4895–4950.
[20] A.-C. Knall, C. Slugovc, Chem. Soc. Rev. 42 (2013) 5131–5142.
[21] Y. Qu, F.-X. Sauvage, G. Clavier, F. Miomandre, P. Audebert, Angew. Chem. Int. Ed. 57 (2018) 12057–12061.
[22] H. Li, Z. Sun, W. Wu, X. Wang, M. Zhang, X. Lu, W. Zhong, D. Dai, Org. Lett. 20 (2018) 7186–7191.
[23] J.C.T. Carlson, L.G. Meimetis, S.A. Hilderbrand, R. Weissleder, Angew. Chem. Int. Ed. 52 (2013) 6917–6920.
[24] H. Dong, C. Chen, H. Zhang, C. Su, L. Ji, Acta Crystallogr. E58 (2004) o1321–o1322.
[25] F.-F. Jian, P. Ren, Acta Crystallogr. E66 (2010) o427.
[26] G.R. Desiraju, Nature 412 (2001) 397–400.
[27] S. Manohar, A. Thakur, R. Bhatia, S. Walia, P. Ponnan, D.S. Rawat, Int. J. Chem. 54B (2015) 1235–1246.